Langmuir

Article

pubs.acs.org/Langmuir

# Adsorption of Water and Butanol in Silicalite-1 Film Studied with *in Situ* Attenuated Total Reflectance–Fourier Transform Infrared Spectroscopy

Amirfarrokh Farzaneh,[†] Ming Zhou,[†] Elisaveta Potapova,[†] Zoltán Bacsik,[‡] Lindsay Ohlin,[†] Allan Holmgren,[†] Jonas Hedlund,[†] and Mattias Grahn*[,†]

[†]Chemical Technology, Luleå University of Technology, SE-971 87 Luleå, Sweden

[‡]Department of Material and Environmental Chemistry, Stockholm University, SE-106 91 Stockholm, Sweden

**ABSTRACT:** Biobutanol produced by, e.g., acetone–butanol–ethanol (ABE) fermentation is a promising alternative to petroleum-based chemicals as, e.g., solvent and fuel. Recovery of butanol from dilute fermentation broths by hydrophobic membranes and adsorbents has been identified as a promising route. In this work, the adsorption of water and butanol vapor in a silicalite-1 film was studied using *in situ* attenuated total reflectance–Fourier transform infrared (ATR–FTIR) spectroscopy to better understand the adsorption properties of silicalite-1 membranes and adsorbents. Single-component adsorption isotherms were determined in the temperature range of 35–120 °C, and the Langmuir model was successfully fitted to the experimental data. The adsorption of butanol is very favorable compared to that of water. When the silicalite-1 film was exposed to a butanol/water vapor mixture with 15 mol % butanol (which is the vapor composition of an aqueous solution containing 2 wt % butanol, a typical concentration in an ABE fermentation broth, i.e., the composition of the gas obtained from gas stripping of an ABE broth) at 35 °C, the adsorption selectivity toward butanol was as high as 107. These results confirm that silicalite-1 quite selectively adsorbs hydrocarbons from vapor mixtures. To the best of our knowledge, this is the first comprehensive study on the adsorption of water and butanol in silicalite-1 from vapor phase.

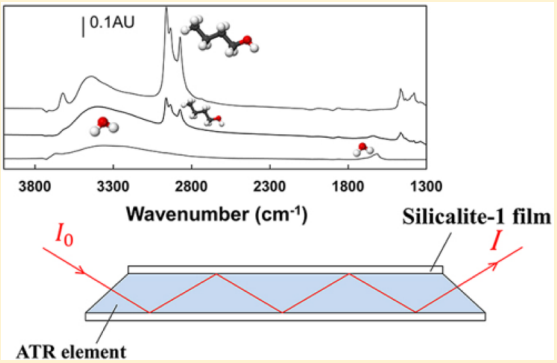


## INTRODUCTION

With the depleting reservoirs of fossil fuels, increasing environmental concerns for flue gas emissions from fossil fuel combustion, and growing world population, the need for new sustainable fuels is higher than ever.[1] Alcohols are important substitutes for the traditional petroleum-based fuels because they can be produced from renewable feedstocks via, for instance, fermentation.[2] Ethanol is already used extensively in the world as fuel in Otto engines,[3] albeit typically as blended in gasoline in varying proportions. 1-Butanol (further referred to as butanol) has great potential as biofuel for Otto engines because of its high octane number of 95 as well as a higher specific energy value than that of ethanol, and in addition, it shows low corrosivity and suitable volatility.[4] Butanol can be produced from sugars by a fermentive process, called acetone–butanol–ethanol (ABE) fermentation, using, e.g., a Clostridia strain of bacteria. The fermentation broth typically contains acetone, butanol, and ethanol in the ratio 3:6:1, where the maximum concentration of butanol is roughly 2 wt % set by the bacteria.[5] At this low concentration of butanol, the energy required to recover butanol by distillation is higher than the energy content of the product itself.[6] Therefore, an efficient separation method for the recovery of butanol from a dilute aqueous solution is a prerequisite for this process to be competitive. The situation can be improved using a so-called gas-stripping ABE fermentation process. Gas stripping is one of the processes that can be a simple process for recovery of liquid fuels, such as butanol. In this process, gas can be sparged through the fermenter and butanol (with a higher concentration compared to the fermentation broth) can be condensed and recovered from the condenser.[7]

Adsorption and membrane separation processes are in general considered as energy-efficient separation processes compared to thermally driven processes, such as distillation, and have also been identified as promising for efficient recovery of biobutanol from ABE fermentation broths.[8] Because of the great potential of butanol, there has recently been an increased interest in developing suitable adsorbents for butanol recovery, with some of the most studied materials including zeolite,[9] activated carbon,[10,11] and polymeric resins.[12,13] Silicalite-1 is the pure silica analogue of the zeolite ZSM-5.[14,15] The absence of aluminum in the crystal makes the material more hydrophobic than ZSM-5.[16] Because of its hydrophobic character, organic compounds, such as methanol, ethanol, acetone, propanol, and

**Received:** February 6, 2015
**Revised:** April 13, 2015
**Published:** April 14, 2015

  

DOI: 10.1021/acs.langmuir.5b00489
*Langmuir* 2015, 31, 4887–4894

butanol, are preferentially adsorbed over water from aqueous solutions. Several groups have studied the adsorption of butanol and other components present in the ABE fermentation broth in silicalite-1[17−19] and low-aluminum ZSM-5[2,20,21] from aqueous solutions. Adsorption on hydrophobic adsorbents, such as silicalite-1,[17,18,20,21] was suggested as a promising technique for recovery of butanol from fermentation broth compared to pervaporation or liquid−liquid extraction. For example, Stoeger et al.[22] studied bioalcohol recovery potential of a pure silica MFI membrane and reported a separation factor of 21 and total flux of 0.11 kg $m^{-2}$ $h^{-1}$ for butanol extraction from an aqueous mixture. Our group has previously investigated the recovery of butanol from dilute aqueous solutions with both adsorbents and membranes. Faisal et al.[23] (also previously Oudshoorn et al.[9]) investigated the recovery of butanol and butyric acid from model and real fermentation broths using high-silica MFI, and it was shown that other species present in the broth, e.g., acetone, ethanol, and acetic acid, only had a minor effect on the amount of butanol or butyric acid adsorbed. The Langmuir isotherm model fitted the experimental data for butanol adsorption in MFI zeolite, and a maximum loading of 1.6 mmol/g was reported for butanol adsorption at room temperature. Zhou et al.[24] evaluated MFI membranes for separation of butanol and water by vapor permeation and reported very high permeance of butanol ($11 \times 10^{-7}$ mol $m^{-2}$ $s^{-1}$ $Pa^{-1}$), with a butanol/water selectivity of 19. Korelskiy et al.[25] reported very high fluxes (up to 4 kg $m^{-2}$ $h^{-1}$) in separation of butanol and water by pervaporation using a hydrophobic MFI membrane with a Si/Al ratio of 139. The aim of the current work was to measure adsorption isotherms of butanol and water in a silicalite-1 film from vapor phase using *in situ* attenuated total reflectance−Fourier transform infrared (ATR−FTIR) spectroscopy. Adsorption data for this system from the vapor phase is scarce but is of great value for understanding the performance of silicalite-1 membranes for pervaporation and vapor permeation processes and also the performance of silicalite-1 adsorbents in gas-phase separation processes. The data could aid the design of a process for separation of butanol from the vapor emanating from a gas stripping of an ABE broth or from a vaporized broth. The ATR−FTIR technique used in this work was developed within the group and has previously been used for studying the adsorption of hydrocarbons (methane, *n*-hexane, and *p*-xylene) and light gases (carbon dioxide and water vapor) in silicalite-1 and ZSM-5 films.[26−29]

## EXPERIMENTAL SECTION

**Film Synthesis and General Characterization.** Thin silicalite-1 films were grown on both sides of a ZnS ATR crystal (with the dimension of 50 × 20 × 2 mm and 45° cut edges, Crystran, Ltd.) using a seeding method. This method has been developed in our group, and details of the procedure can be found elsewhere.[30−32] However, the method will be briefly explained here. Silicalite-1 seed crystals were synthesized from a mixture of tetraethoxysilane (TEOS, 99%, Merck), tetrapropylammonium hydroxide (TPAOH, AppliChem, 40 wt % aqueous solution), and water by hydrolysis for 1 day, followed by hydrothermal treatment at 130 °C for 9 h under constant stirring. The molar composition of the synthesis mixture was 1.00 TEOS/0.200 TPAOH/100 $H_2O$. The synthesized crystals were separated from the supernatant by repetitive centrifugation, and after each step, the crystals were redispersed in doubly distilled water.[30]

To facilitate the attachment of the seeds to the ATR crystal, both sides of the ATR crystal were coated by a thin layer of cellulosic polymer [hydroxypropylcellulose (HPC), Sigma-Aldrich, 99%] using a spin coater (2% HPC dissolved in ethanol solution, and the spin coating was conducted at 3000 rpm for 15 s).[31] After drying at 105 °C for 1 h, a monolayer of silicalite-1 crystals was assembled on the ATR crystal by rubbing the powder of seeds onto both surfaces.[32] The seeded ATR crystal was calcined at 500 °C for 2 h with a heating and cooling rate of 0.8 °C/min to remove the polymer layer between the silicalite seeds and the ATR crystal. Thereafter, the seeded ATR crystal was kept for 5 h in a synthesis solution, which was prehydrolyzed for 12 h on a shaker, with a molar composition of 1.00 TEOS/0.0500 TPAOH/165 $H_2O$ in an autoclave at 150 °C to grow the seed crystals into a continuous silicalite-1 film. After synthesis, the film was thoroughly rinsed with a 0.1 M ammonia solution and dried at 50 °C overnight. The film was subsequently calcined at 500 °C for 2 h with a heating and cooling rate of 0.8 °C/min to remove the template molecules from the pores of the zeolite.

For the characterization of the film, scanning electron microscopy (SEM) images were recorded using a Magellan 400 (FEI Company, Eindhoven, Netherlands) microscope, and X-ray diffraction (XRD) patterns were recorded using a PANalytical Empyrean instrument, equipped with a PIXcel3D detector and a Cu LFF HR X-ray tube.

***In Situ* ATR−FTIR Experiments.** The ATR−FTIR spectra were recorded on a Bruker IFS66v/S FTIR spectrometer equipped with a deuterated triglycine sulfate (DTGS) detector. Each spectrum was obtained by averaging 256 scans at a resolution of 4 $cm^{-1}$. The ATR crystal was mounted in a steel flow cell connected to a gas delivery system, which has been described in detail previously.[33] Prior to the adsorption experiment, the silicalite-1-film-coated ATR crystal was mounted in the cell and dried under a constant flow rate of helium at 300 °C for 4 h. The heating and cooling rates were 0.9 °C/min. A background spectrum of the dried film was recorded under helium flow at the desired experimental temperature prior to the adsorption measurements. After the background was recorded, the adsorption experiment was carried out by introducing butanol or water to the helium flow and recording spectra at equilibrium. The helium carrier gas was fed to two saturators connected in series and filled with either water or butanol or a butanol/water mixture. The temperature of the second saturator was always lower than that of the first saturator, and the cooling was controlled by a cooling jacket connected to a circuit of glycol. The saturated helium stream was thereafter diluted with an appropriate amount of helium to arrive at the desired partial pressure. The total pressure was 1 atm in all measurements. In an ATR experiment, the Beer−Lambert law is not directly applicable because of the experimental conditions; however, Mirabella et al.[34] and Tompkins et al.[35] have shown that the concentration of components adsorbed in a film deposited on an ATR crystal can be determined from eq 1

$$\frac{A}{N} = \frac{n_{21} E_0^{\,2} \varepsilon}{\cos\theta} \int_0^\infty C(z)^{-2z/d_p}\, \mathrm{d}_z \qquad (1)$$

where $A$ represents the integrated absorbance of a characteristic absorption band in the infrared (IR) spectrum, $N$ is the number of reflections (20) inside the ATR element between the gaskets sealing of the cell, and $n_{21}$ is the ratio of the refractive indices of the ZnS ATR crystal and silicalite-1 film. The refractive index of ZnS is ca. 2.25, whereas Tsapatsis and Nair[36] reported the refractive index of empty MFI zeolite films in the IR region of 3000−1500 $cm^{-1}$. As water or butanol adsorbs in the film, the refractive index of the film will change, and to compensate for this, it was assumed that the refractive index of the film changed linearly with adsorbed loading. Further, $E_0$ is the amplitude of the electric field at the film−ATR crystal interface,[26,29] and $\varepsilon$ is the molar absorptivity, which was determined for water by Ohlin et al.[28] for a high-silica (Si/Al = 130) film. $\theta$ is the angle of incidence (45°), and $C(z)$ is the concentration of an adsorbate in the film. Further, $d_p$ is the penetration depth, which is defined as the distance required for the electric field amplitude to fall to $e^{-1}$ of its value at the surface and is calculated using eq 2.

$$d_p = \frac{\lambda_1}{2\pi(\sin^2\theta - n_{21}^{\,2})^{1/2}} \qquad (2)$$



DOI: 10.1021/acs.langmuir.5b00489
*Langmuir* 2015, 31, 4887−4894

In this equation, $\lambda_1$ is the wavelength of the IR radiation in the ATR element. After integrating eq 1 over the film thickness, assuming a homogeneous concentration of the adsorbate in the film at equilibrium, and neglecting the absorbance from the adsorbate in the bulk gas outside the film, a reasonable assumption as shown previously[26] (eq 3) is obtained.

$$\frac{A}{N} = \frac{n_{21}E_0^{\ 2}d_pC}{2\cos\theta}\varepsilon(1 - e^{-2d_a/d_p}) \quad (3)$$

Here, $d_a$ is the thickness of the silicalite film.

To use the Beer–Lambert law for the data obtained from ATR–FTIR, "effective thickness" ($d_e$) was introduced as

$$d_e = \frac{n_{21}E_0^{\ 2}d_p}{2\cos\theta} \quad (4)$$

which is the distance required to reach the same absorbance in a transmission experiment as in an ATR experiment, and it was described in detail previously.[26,34]

The butanol/water selectivity of the silicalite-1 film was also determined by exposing the film to a gas mixture with a molar composition of 15% butanol and 85% water at 35 °C. The adsorption selectivity was calculated using eq 5

$$\alpha_{BuOH/H_2O} = \frac{X_{BuOH}/X_{H_2O}}{Y_{BuOH}/Y_{H_2O}} \quad (5)$$

where $X$ is the mole fraction of an adsorbate in the film and $Y$ is the mole fraction of an adsorbate in the feed.

**Adsorption of Butanol in Silicalite-1 Powder.** The adsorption isotherm of butanol from the vapor phase in silicalite-1 powder at 35 °C were determined using an ASAP 2020 gas adsorption instrument (Micromeritics, Norcross, GA). Prior to the adsorption measurements, the sample was dried under dynamic vacuum conditions (<0.1 mPa) at 300 °C for 4 h with heating and cooling rates of 1 °C/min. The temperature was controlled by immersing the sample in a Dewar flask coupled to a refrigerating and heating circulator (Julabo, Germany).

Because the molar absorptivity for butanol adsorbed in silicalite-1 is not yet reported, it was assumed that the silicalite-1 film had the same saturation capacity for butanol as the silicalite-1 powder.[37] Hammond et al.[38] compared the adsorption behavior of a MFI membrane to that of a MFI powder and drew the conclusion that the adsorption behavior for the two samples was very similar and that the adsorption behavior of the membrane could safely be approximated to that of the corresponding powder. Moreover, because the saturation loading of butanol in MFI is dictated by how many molecules may fit per unit cell, it that should be very similar for both powder and films. Strain in the zeolite film may possibly affect the pore volume.[39,40] However, considering that the kinetic diameter of 1-butanol (4.4 Å) is considerably smaller than the pore diameter of MFI (5.5 Å), strain is unlikely to affect the saturation loading, and even if the saturation capacity was reduced by strain by reducing the pore volume, the same should apply to water, leading to only a minor effect on the adsorption selectivity. The maximum absorbance determined for butanol from IR spectra of the butanol-loaded silicalite-1 film was assumed to correspond to the maximum adsorbed loading of butanol determined by the volumetric adsorption measurements on the silicalite-1 powder. It should be noted that the saturation capacity of the powder was determined below the mesoporous region ($P/P_0$ = 0.15) to avoid contribution from any butanol capillary condensating between the powder grains.

## RESULT AND DISCUSSION

**Film Characterization.** Panels a and b of Figure 1 show SEM images of the surface of an ATR crystal coated with a monolayer of silicalite-1 seeds. A closely packed and uniformly b-oriented layer of silicalite-1 seeds covered the ATR crystal, and no polymer layer was present between the layer of the seeds and the ATR element after calcination. Top- and side-view SEM images of the silicalite-1 film after synthesis are shown in panels c and d of Figure 1. These images show that the seed crystals grew uniformly without secondary nucleation and formed a dense layer of b-oriented crystals with a thickness of approximately 750 nm. After a thorough examination by SEM, neither cracks nor pinholes could be observed.

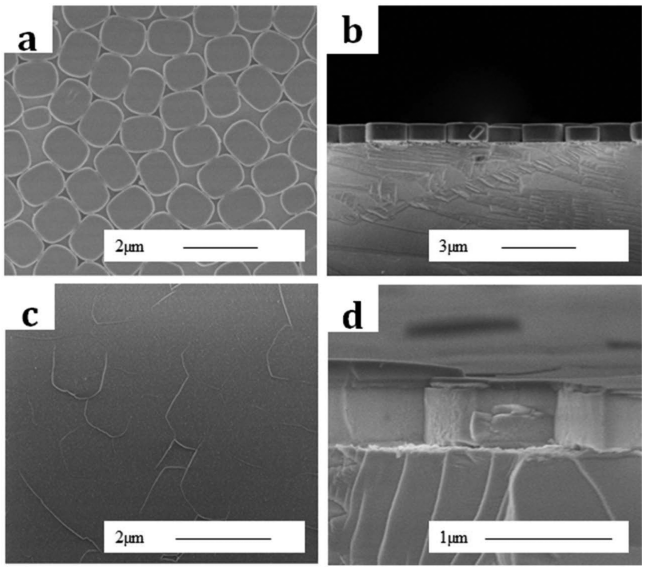


**Figure 1.** (a and c) Top-view and (b and d) side-view SEM images of the (a and b) silicalite-1 seed layer and (c and d ) grown film.

Figure 2 shows an XRD pattern of an ATR crystal coated by a silicalite-1 film after growth in the synthesis solution. The pattern shows that the film consists of b-oriented crystals as merely reflections from (0 $k$ 0) planes observed. This is in agreement with the SEM observations, showing that the seed crystals were b-oriented and that these crystals grew to a uniform film without any secondary nucleation. Weaker reflections emanating from the ZnS support are observed at $2\theta$ of 28.5° and 47.5° in the pattern as well. These results are in very good agreement with previous findings.[30,41]

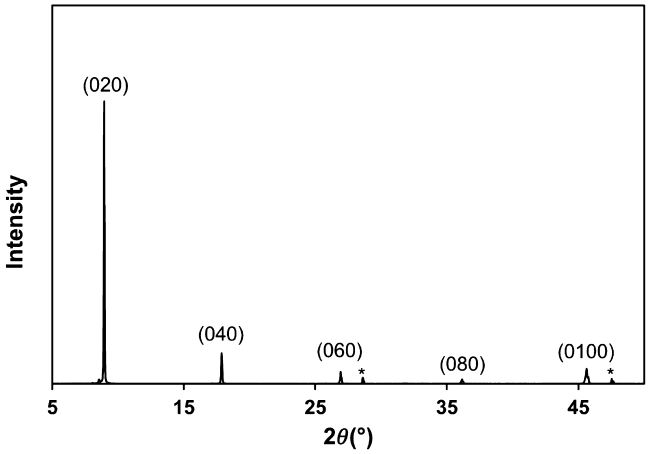


**Figure 2.** XRD pattern of a silicalite-1 film synthesized on a ZnS crystal in the $2\theta$ range of 5–50°. The indexed reflections emanate from the film comprised of b-oriented crystals, and the reflections labeled "*" represent the ZnS crystal.

**ATR–FTIR Adsorption Experiments.** *Water.* Figure 3 shows IR spectra of water adsorbed in the silicalite-1 film at 35



DOI: 10.1021/acs.langmuir.5b00489
Langmuir 2015, 31, 4887–4894

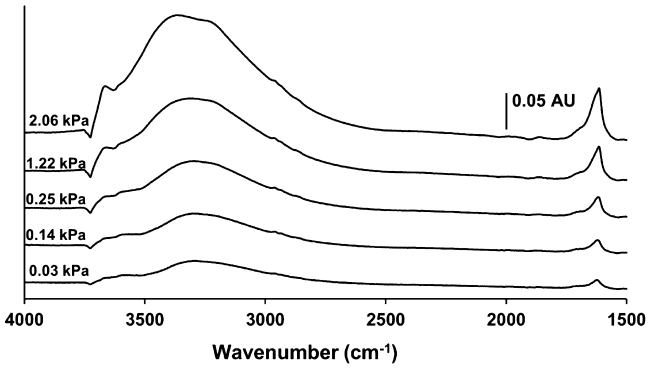


**Figure 3.** IR spectra of water adsorbed in silicalite-1 at 35 °C at different partial pressures.

°C and various partial pressures. Two main bands assigned to adsorbed water appear in the spectra. The broad band in the range of 3700−2700 $cm^{-1}$ originates from the O−H stretching vibration modes (asymmetric and symmetric) in adsorbed water, and the band at ca. 1620 $cm^{-1}$ is assigned to the bending vibration of water.[42,43] The peak value of the bending vibration band was observed at a lower wavenumber than the same vibration mode in bulk water (ca. 1650 $cm^{-1}$), which indicates that the interaction between water molecules and the zeolite surface was weaker than the interaction between water molecules in liquid water. Further, a negative band was observed at 3730 $cm^{-1}$, which was previously assigned to the O−H stretching vibration of free silanol groups.[44] When water adsorbs on the silanol groups, the intensity of this band decreased and a downshifted broader band appears for H-bonded silanol groups (partially overlapped by the OH bands of water). As expected, the intensity of the bands assigned to adsorbed water increases with increasing partial pressure in the feed, showing that the amount of adsorbed water increases with an increasing partial pressure in the feed. The spectra are typical for water adsorbed in zeolite and very similar to the spectra reported previously by, e.g., Ohlin et al.,[28] Jentys et al.,[44] and Rege et al.[45]

The amount of water adsorbed in the zeolite at different partial pressures of water was determined from the recorded IR spectra by integrating the area of the O−H band at 1620 $cm^{-1}$ and calculating the corresponding loadings using eq 3. Ohlin et al.[28] determined the molar absorptivity ($\varepsilon$) for the same band of water adsorbed in the ZSM-5 to 0.654 cm/$\mu$mol using a method for combined analysis by gravimetry and infrared spectroscopy (AGIR).[46] This value was assumed to be valid in this work, and this assumption should be reasonable because the ZSM-5 film used by Ohlin et al.[28] had a very low aluminum content (Si/Al = 130) and should, therefore, show similar properties to the silicalite-1 film used in this work.

Figure 4 shows the adsorption isotherms of water in silicalite-1 derived from the IR spectra and using eq 3. Only isotherms recorded at 35, 50, and 85 °C are shown because no signal from adsorbed water was observed at 120 °C. The isotherms at lower temperatures show a steep increase in loading at low partial pressures, corresponding to adsorption of water on the high-energy sites, but at higher partial pressures, the slope of the isotherms is decreased and the maximum loading is not reached at any of the temperatures at the conditions (e.g., partial pressure of water in the gas phase) studied in this work. As expected, the amount adsorbed decreased rapidly with increasing temperature and the adsorption isotherm recorded

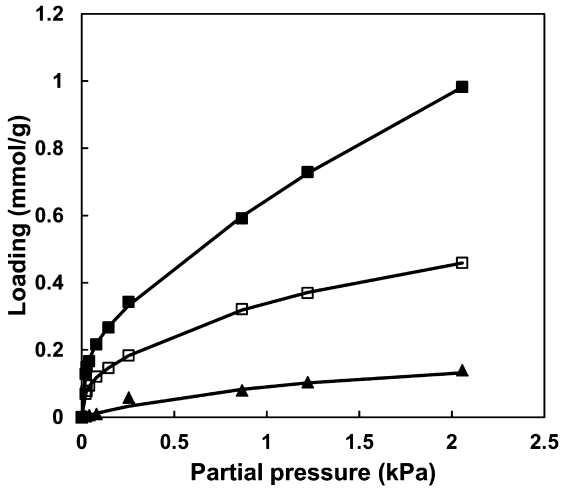


**Figure 4.** Adsorption isotherms for water in the silicalite-1 film determined at (■) 35 °C, (□) 50 °C, and (▲) 85 °C. Symbols present the experimental data, and solid lines represent the dual-site Langmuir model fitted to the experimental data.

at 85 °C shows little adsorption. The dual-site Langmuir model (eq 6) was fitted to the experimental data

$$q_{tot} = q_1 \frac{b_1 p}{1 + b_1 p} + q_2 \frac{b_2 p}{1 + b_2 p} \quad (6)$$

where $q_1$ and $q_2$ are the saturation loadings of the sites (mmol/g), $p$ is the partial pressure of adsorbate in the gas phase (kPa), and $b_1$ and $b_2$ are the Langmuir adsorption coefficients ($kPa^{-1}$) for each site. The fitted parameters determined in the present work are shown in Table 1. The fitted data at 35 and 50 °C

**Table 1. Saturation Loadings ($q_{sat}$, mmol/g) and Langmuir Adsorption Parameters ($b_i$, $kPa^{-1}$) for Water and Butanol in Silicalite-1**

| adsorbate | temperature (°C) | $q_1$ (mmol/g) | $b_1$ ($kPa^{-1}$) | $q_2$ (mmol/g) | $b_2$ ($kPa^{-1}$) |
|---|---|---|---|---|---|
| water | 35 | 0.23 | 48.38 | 2.96 | 0.17 |
| | 50 | 0.23 | 12.14 | 2.96 | 0.04 |
| | 85 | 0.23 | 3.43 | | |
| butanol | 35 | 1.8 | 860 | | |
| | 50 | 1.8 | 267 | | |
| | 85 | 1.8 | 15.6 | | |
| | 120 | 1.8 | 2.6 | | |

show a site with the maximum loading of 2.96 mmol/g and very low affinities (see Table 1). Therefore, it was assumed that water molecules cannot adsorb at that site at 85 °C, and the Langmuir data were fitted to a maximum loading of 0.23 mmol/g at 85 °C.

The fitted saturation loading ($q_1 + q_2$) of 3.2 mmol/g in the present work is close to the saturation loadings reported previously for water adsorbed in silicalite-1 and ZSM-5 with a high Si/Al ratio.[47,48] For example, Zhang et al.[49] reported maximum loadings of water in silicalite-1, $NH_4$-ZSM5, and H-ZSM5 zeolites with Si/Al of 140 ranging between 2 and 3 mmol/g. Our values of $b_1$ and $b_2$ for silicalite-1 at 35, 50, and 85 °C are lower than those reported by Ohlin et al.[28] for Na-ZSM-5 zeolite with a Si/Al ratio of 130, which shows that silicalite-1 has lower affinity for water, i.e., is less hydrophilic compared to Na-ZSM-5.



DOI: 10.1021/acs.langmuir.5b00489
*Langmuir* 2015, 31, 4887−4894

Table 2. Heat of Adsorption for Butanol and Water in This Work and from Literature Data

| adsorbate | adsorbent | $\Delta H_{ads}$ (kJ/mol) | reference |
|---|---|---|---|
| water | silicalite-1 | −79 (site 1) | this work |
| | | −46 (site 2) | |
| | Na-ZSM-5 | −72 (site 1) | Ohlin et al.[28] |
| | | −58 (site 2) | |
| | silicalite-1 | −68 | Bolis et al.[48] |
| | silicalite-1 | −46 | Zhang et al.[49] |
| | H-ZSM-5 | −75 | Olson et al.[47] |
| butanol | silicalite-1 | −69 | this work |
| | ZIF-8 | −40 | Zhang et al.[53] |
| | | −50 | Einicke et al.[54] |
| | silicalite-1 (for butane isomers) | −56 | Zhu et al.[55] |

The Langmuir parameters are related to the heat of adsorption ($\Delta H_{ads}$), reflecting the affinity of the adsorbate for the adsorbent surface. The limiting heat of adsorption was determined using the van't Hoff equation from the linear region of the isotherms

$$\ln b = -\frac{\Delta H_{ads}}{RT} + \frac{\Delta S_{ads}}{R} \quad (7)$$

where $\Delta S_{ads}$ is the entropy change upon the adsorption, $R$ is the gas constant, and $T$ is the absolute temperature. Table 2 shows the values for heat of adsorption for water determined in the present work together with the values previously reported in the literature. The values of −79 and −46 kJ/mol for sites 1 and 2, respectively, obtained in the present work are comparable to previously reported results. Bolis et al.[41] and Zhang et al.[42] reported values of heat of adsorption in silicalite-1 to −68 and −46 kJ/mol, respectively. Olson et al.[40] reported the heat of adsorption for water in H-ZSM-5 with a Si/Al ratio of 38 to −113 kJ/mol. Ohlin et al.[27] used the same experimental setup as used in the present work and determined the heat of adsorption for water in Na-ZSM-5 with a Si/Al ratio of 130 to −72 and −58 kJ/mol for the two sites, respectively. These latter results are quite close to the results obtained in the present work.

*Butanol.* Figure 5 shows IR spectra of butanol adsorbed in the silicalite-1 film at 35 °C with different partial pressures of butanol in the feed. The intensity of the bands increase with increasing partial pressures, indicating increased adsorption with increasing partial pressure of butanol in the feed. The spectra recorded during butanol adsorption contain the characteristic $CH_3$ and $CH_2$ stretching vibration bands at 3000−2800 $cm^{-1}$ originating from butanol adsorbed in silicalite-1 film.[50,51] The bands at 1380 and 1465 $cm^{-1}$ were assigned to the $CH_3$ and $CH_2$ bending vibrations. The broad band in the range of 3700−2700 $cm^{-1}$ originates from the O−H stretching vibration in adsorbed butanol. A negative band at 3730 $cm^{-1}$ is associated with the decreasing amount of free silanol groups because they interact with butanol adsorbed.

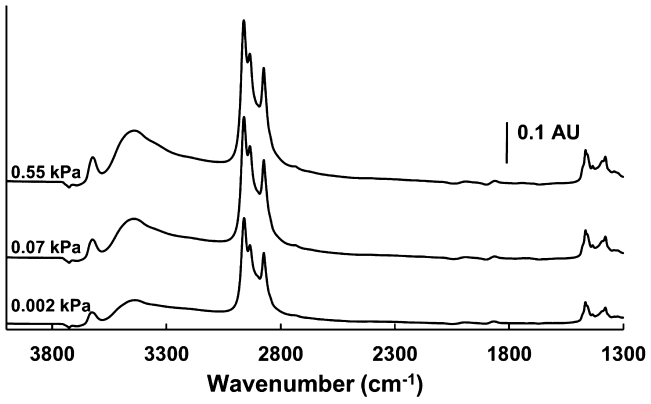


Figure 5. IR spectra of butanol adsorbed in silicalite-1 at 35 °C at different partial pressures.

Figure 6 shows the adsorption isotherms of butanol in silicalite-1 in the temperature range of 35−120 °C extracted from the IR spectra together with the fitted single-site Langmuir adsorption model (eq 8).

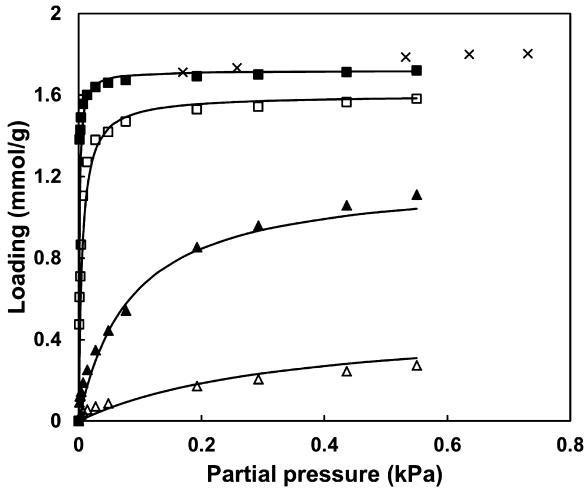


Figure 6. Adsorption isotherms for butanol in silicalite-1 film at (■) 35 °C, (□) 50 °C, (▲) 85 °C, and (△) 120 °C, obtained from FTIR experiments and in silicalite-1 powder at 35 °C (×) obtained from volumetric measurements. Symbols present the experimental data, and solid lines represent the single-site Langmuir model fitted to the experimental data.

$$q = q_m \frac{bp}{1 + bp} \quad (8)$$

The isotherms are typical for adsorption in microporous materials and are very similar to previous reported isotherms of butanol in silicalite-1.[9,20,52] The Langmuir data were fitted to a maximum loading of 1.7 mmol/g, which is the plateau value for the isotherm at 35 °C in Figure 6. This value for maximum loading was obtained from the isotherms determined for silicalite-1 powder at 35 °C using the volumetric gas adsorption technique (also presented in Figure 6). The isotherm obtained



DOI: 10.1021/acs.langmuir.5b00489
Langmuir 2015, 31, 4887−4894

from the volumetric gas adsorption measurement (×) shows that the loading of butanol in silicalite-1 was increasing slowly at high pressures, resulting in adsorbed loadings higher than 1.7 mmol/g at partial pressures closer to the saturated vapor pressure of butanol at 35 °C ($P^*$ = 1.8 kPa). This is probably due to capillary condensation in the voids between the crystals of the silicalite-1 powder.

In general, the single-site Langmuir adsorption model fits the data well; however, for the two highest temperatures, there is some discrepancy between the model and experimental data, probably because of the presence of a few high-energy adsorption sites as evident by the sharp increase in loadings at low pressures also at these high temperatures. The fitted parameters are listed in Table 2 together with values previously reported in the literature. According to the previous studies,[2,5,9,19,21,23] the maximum loadings of butanol in silicalite-1 and MFI zeolites are reported in the range of 0.7−2.5 mmol/g. The inconsistency is probably due to the different experimental conditions and samples used. However, most of the values reported are in the range of 1.3−2 mmol/g. As shown in Figure 6, the maximum loading according to the present work was 1.7 mmol/g (determined using a volumetric gas adsorption analyzer), which is in the range of the literature data.

The heat of adsorption was determined to be −69 kJ/mol using the van't Hoff equation (eq 7) from all four temperatures. The fit was very good, with a $R^2$ value of 0.998.

There are only few reports on the heat of adsorption for butanol in hydrophobic adsorbents in the literature. However, the heat of adsorption calculated in the present work is in good agreement with the previous findings reported by Einicke et al.[54] and Zhang et al.[53] (−49.6 and −40 kJ/mol, respectively). Several papers reported the heat of adsorption of butane (which should have a reasonable similar adsorption behavior as butanol in hydrophobic adsorbents) in silicalite-1 in the range from −50 to −60 kJ/mol,[55−58] which is also in a good agreement with the present work.

*Adsorption of Butanol and Water from a Binary Mixture.* By considering the single-component adsorption results, it would be expected that butanol would be preferentially adsorbed in silicalite-1 from a butanol/water vapor mixture. A number of experiments were carried out with simultaneous adsorption of water and butanol at 35 °C with partial pressures in the feed of 2.04 and 0.35 kPa for water and butanol (with a molar composition of 15% butanol), respectively. The partial pressures of water and butanol vapor in the feed gas were obtained by passing the carrier gas (helium) to saturators filled with a dilute butanol/water mixture containing 2 wt % butanol, i.e., a typical concentration in an ABE fermentation broth. In other words, these conditions simulate a gas-stripping ABE fermentation process.[21,52] Figure 7 shows IR spectra recorded of the butanol and water adsorbed simultaneously in the silicalite-1 film at 35 °C as well as reference spectra of water and butanol adsorbed from the single-component measurements for visualization of the difference between single-component and binary mixture adsorption. The reference spectra were recorded at the partial pressures close to those in the mixture, viz., 2.06 kPa for water and 0.05 kPa for butanol. Both the characteristic band of water at 1620 $cm^{-1}$ and the band assigned to butanol at 1465 $cm^{-1}$ are visible and clearly separated in the spectrum recorded for the binary mixture. The bands assigned to water are significantly smaller than the bands in the reference spectrum, whereas the difference is much smaller in the case of butanol. This observation clearly shows that the silicalite-1 film is selective toward butanol. The adsorption selectivity, as determined by extracting the adsorbed concentrations from the spectrum using eqs 3 and 4, was $\alpha_{BuOH/water}$ = 107, showing that the film is highly butanol-selective at these conditions. By increasing the partial pressure of butanol in the feed, butanol/water selectivity was measured also at feed compositions, 2.03 kPa water and 0.57 kPa butanol and 1.80 kPa water and 0.70 kPa butanol, which resulted in selectivities of 84 and 62, respectively. The lower selectivities at higher feed pressures may be expected, because silicalite-1 was already saturated by butanol at low partial pressures. Unfortunately, only a few reports exist in the literature on the adsorption selectivity for adsorption of a butanol/water vapor mixture in zeolites. However, Zhang et al.[59] reported butanol adsorption selectivity in the range of 12−60 and 15−80 (at different mole fractions of butanol in the liquid phase) for ZIF-8 and ZIF-71 zeolitic imidazolates, respectively. The high butanol selectivity obtained in the present work indicates that recovery of butanol from the vapor phase from a gas-stripping ABE fermentation process may be an interesting option.

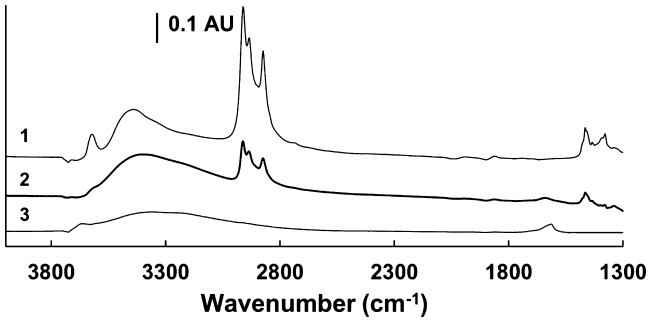


**Figure 7.** IR spectrum of butanol and water adsorbed in silicalite-1 film at 35 °C for a binary mixture of butanol and water with a mole fraction of 0.15 for butanol in the vapor phase (2), together with the spectra of pure butanol (1) and water (3) at partial pressures of 0.05 and 2.06 kPa, respectively.

## CONCLUSION

The adsorption of butanol and water in silicalite-1 was studied and quantitatively determined at four different temperatures using ATR−FTIR spectroscopy. The adsorption was typical for microporous materials, and the Langmuir model was found to fit well to the experimental data. The Langmuir parameters, heats of adsorption, and maximum loadings determined were in a good agreement with previously reported data. The saturation concentration of butanol in silicalite-1 powder was measured using a volumetric gas adsorption technique, and the amount of butanol and water adsorbed in the silicalite-1 film were determined from IR spectra. Moreover, it was shown that the silicalite-1 film was butanol-selective with an adsorption selectivity of 107 at 35 °C when adsorbed from a binary vapor mixture with the molar composition of 15% butanol and 85% water. The results indicate that a silicalite-1 adsorbent or membrane may effectively separate butanol from the vapor obtained in an ABE fermentation gas-stripping process.

## AUTHOR INFORMATION

### Corresponding Author

*E-mail: mattias.grahn@ltu.se.



DOI: 10.1021/acs.langmuir.5b00489
*Langmuir* 2015, 31, 4887−4894

### Notes

The authors declare no competing financial interest.

## ■ ACKNOWLEDGMENTS

The authors acknowledge the Swedish Research Council (VR, under Grant 621-2011-4060) for financially supporting this work.

## ■ REFERENCES

(1) Yuan, J. S.; Tiller, K. H.; Al-Ahmad, H.; Stewart, N. R.; Stewart, C. N., Jr. Plants to power: Bioenergy to fuel the future. *Trends Plant Sci.* **2008**, *13*, 421−429.
(2) Saravanan, V.; Waijers, D.; Ziari, M.; Noordermeer, M. Recovery of 1-butanol from aqueous solutions using zeolite ZSM-5 with a high Si/Al ratio; suitability of a column process for industrial applications. *Biochem. Eng. J.* **2010**, *49*, 33−39.
(3) Demirbas, A. *Biodiesel*; Springer: New York, 2008.
(4) Crabbe, E.; Nolasco-Hipolito, C.; Kobayashi, G.; Sonomoto, K.; Ishizaki, A. Biodiesel production from crude palm oil and evaluation of butanol extraction and fuel properties. *Process Biochem.* **2001**, *37*, 65−71.
(5) Qureshi, N.; Hughes, S.; Maddox, I.; Cotta, M. Energy-efficient recovery of butanol from model solutions and fermentation broth by adsorption. *Bioprocess Biosyst. Eng.* **2005**, *27*, 215−222.
(6) García, V.; Päkkilä, J.; Ojamo, H.; Muurinen, E.; Keiski, R. L. Challenges in biobutanol production: How to improve the efficiency? *Renewable Sustainable Energy Rev.* **2011**, *15*, 964−980.
(7) Ezeji, T.; Qureshi, N.; Blaschek, H. Acetone butanol ethanol (ABE) production from concentrated substrate: Reduction in substrate inhibition by fed-batch technique and product inhibition by gas stripping. *Appl. Microbiol. Biotechnol.* **2004**, *63*, 653−658.
(8) Liu, F.; Liu, L.; Feng, X. Separation of acetone−butanol−ethanol (ABE) from dilute aqueous solutions by pervaporation. *Sep. Purif. Technol.* **2005**, *42*, 273−282.
(9) Oudshoorn, A.; van der Wielen, L. A. M.; Straathof, A. J. Adsorption equilibria of bio-based butanol solutions using zeolite. *Biochem. Eng. J.* **2009**, *48*, 99−103.
(10) Nielsen, L.; Larsson, M.; Holst, O.; Mattiasson, B. Adsorbents for extractive bioconversion applied to the acetone−butanol fermentation. *Appl. Microbiol. Biotechnol.* **1988**, *28*, 335−339.
(11) Giusti, D.; Conway, R.; Lawson, C. Activated carbon adsorption of petrochemicals. *J.—Water Pollut. Control Fed.* **1974**, 947−965.
(12) Nielsen, D. R.; Prather, K. J. *In situ* product recovery of *n*-butanol using polymeric resins. *Biotechnol. Bioeng.* **2009**, *102*, 811−821.
(13) Lin, X.; Wu, J.; Fan, J.; Qian, W.; Zhou, X.; Qian, C.; Jin, X.; Wang, L.; Bai, J.; Ying, H. Adsorption of butanol from aqueous solution onto a new type of macroporous adsorption resin: Studies of adsorption isotherms and kinetics simulation. *J. Chem. Technol. Biotechnol.* **2012**, *87*, 924−931.
(14) Szostak, R.; Nair, V.; Thomas, T. L. Incorporation and stability of iron in molecular-sieve structures. Ferrisilicate analogues of zeolite ZSM-5. *J. Chem. Soc., Faraday Trans. 1* **1987**, *83*, 487−494.
(15) Wang, Z.; Larsson, M. L.; Grahn, M.; Holmgren, A.; Hedlund, J. Zeolite coated ATR crystals for new applications in FTIR−ATR spectroscopy. *Chem. Commun. (Cambridge, U. K.)* **2004**, 2888−2889.
(16) Stelzer, J.; Paulus, M.; Hunger, M.; Weitkamp, J. Hydrophobic properties of all-silica zeolite beta. *Microporous Mesoporous Mater.* **1998**, *22*, 1−8.
(17) Huang, J.; Meagher, M. Pervaporative recovery of *n*-butanol from aqueous solutions and ABE fermentation broth using thin-film silicalite-filled silicone composite membranes. *J. Membr. Sci.* **2001**, *192*, 231−242.
(18) Qureshi, N.; Meagher, M.; Huang, J.; Hutkins, R. Acetone butanol ethanol (ABE) recovery by pervaporation using silicalite−silicone composite membrane from fed-batch reactor of *Clostridium acetobutylicum*. *J. Membr. Sci.* **2001**, *187*, 93−102.
(19) Zhou, H.; Su, Y.; Chen, X.; Wan, Y. Separation of acetone, butanol and ethanol (ABE) from dilute aqueous solutions by silicalite-1/PDMS hybrid pervaporation membranes. *Sep. Purif. Technol.* **2011**, *79*, 375−384.
(20) Masuda, T.; Otani, S.; Tsuji, T.; Kitamura, M.; Mukai, S. R. Preparation of hydrophilic and acid-proof silicalite-1 zeolite membrane and its application to selective separation of water from water solutions of concentrated acetic acid by pervaporation. *Sep. Purif. Technol.* **2003**, *32*, 181−189.
(21) Qureshi, N.; Meagher, M.; Hutkins, R. Recovery of butanol from model solutions and fermentation broth using a silicalite/silicone membrane. *J. Membr. Sci.* **1999**, *158*, 115−125.
(22) Stoeger, J. A.; Choi, J.; Tsapatsis, M. Rapid thermal processing and separation performance of columnar MFI membranes on porous stainless steel tubes. *Energy Environ. Sci.* **2011**, *4*, 3479−3486.
(23) Faisal, A.; Zarebska, A.; Saremi, P.; Korelskiy, D.; Ohlin, L.; Rova, U.; Hedlund, J.; Grahn, M. MFI zeolite as adsorbent for selective recovery of hydrocarbons from ABE fermentation broths. *Adsorption* **2014**, *20*, 465−470.
(24) Zhou, H.; Korelskiy, D.; Sjöberg, E.; Hedlund, J. Ultrathin hydrophobic MFI membranes. *Microporous Mesoporous Mater.* **2013**, *192*, 76−81.
(25) Korelskiy, D.; Leppäjärvi, T.; Zhou, H.; Grahn, M.; Tanskanen, J.; Hedlund, J. High flux MFI membranes for pervaporation. *J. Membr. Sci.* **2013**, *427*, 381−389.
(26) Grahn, M.; Holmgren, A.; Hedlund, J. Adsorption of *n*-hexane and *p*-xylene in thin silicalite-1 films studied by FTIR/ATR spectroscopy. *J. Phys. Chem. C* **2008**, *112*, 7717−7724.
(27) Ohlin, L.; Grahn, M. Detailed investigation of the binary adsorption of carbon dioxide and methane in zeolite Na-ZSM-5 studied using *in situ* ATR−FTIR spectroscopy. *J. Phys. Chem. C* **2014**, *118*, 6207−6213.
(28) Ohlin, L.; Bazin, P.; Thibault-Starzyk, F.; Hedlund, J.; Grahn, M. Adsorption of CO2, CH4, and H2O in Zeolite ZSM-5 Studied Using In Situ ATR-FTIR Spectroscopy. *J. Phys. Chem. C* **2013**, *117*, 16972−16982.
(29) Grahn, M.; Lobanova, A.; Holmgren, A.; Hedlund, J. Orientational analysis of adsorbates in molecular sieves by FTIR/ATR spectroscopy. *Chem. Mater.* **2008**, *20*, 6270−6276.
(30) Zhou, M.; Korelskiy, D.; Ye, P.; Grahn, M.; Hedlund, J. A uniformly oriented MFI membrane for improved $CO_2$ separation. *Angew. Chem., Int. Ed.* **2014**, *53*, 3492−3495.
(31) Zhou, M.; Grahn, M.; Zhou, H.; Holmgren, A.; Hedlund, J. The facile assembly of nanocrystals by optimizing humidity. *Chem. Commun.* **2014**, *50*, 14261−14264.
(32) Li, X.; Peng, Y.; Wang, Z.; Yan, Y. Synthesis of highly b-oriented zeolite MFI films by suppressing twin crystal growth during the secondary growth. *CrystEngComm* **2011**, *13*, 3657−3660.
(33) Grahn, M.; Wang, Z.; Lidström-Larsson, M.; Holmgren, A.; Hedlund, J.; Sterte, J. Silicalite-1 coated ATR elements as sensitive chemical sensor probes. *Microporous Mesoporous Mater.* **2005**, *81*, 357−363.
(34) Mirabella, F. M. *Internal Reflection Spectroscopy: Theory and Applications*; CRC Press: Boca Raton, FL, 1992; Vol. *15*.
(35) Tompkins, H. G. The physical basis for analysis of the depth of absorbing species using internal reflection spectroscopy. *Appl. Spectrosc.* **1974**, *28*, 335−341.
(36) Nair, S.; Tsapatsis, M. Infrared reflectance measurements of zeolite film thickness, refractive index and other characteristics. *Microporous Mesoporous Mater.* **2003**, *58*, 81−89.
(37) Bowen, T. C.; Noble, R. D.; Falconer, J. L. Fundamentals and applications of pervaporation through zeolite membranes. *J. Membr. Sci.* **2004**, *245*, 1−33.
(38) Hammond, K. D.; Hong, M.; Tompsett, G. A.; Auerbach, S. M.; Falconer, J. L.; Conner, W. C. High-resolution physical adsorption on supported borosilicate MFI zeolite membranes: Comparison with powdered samples. *J. Membr. Sci.* **2008**, *325*, 413−419.



DOI: 10.1021/acs.langmuir.5b00489
*Langmuir* 2015, 31, 4887−4894

(39) Jeong, H.; Lai, Z.; Tsapatsis, M.; Hanson, J. C. Strain of MFI crystals in membranes: An *in situ* synchrotron X-ray study. *Microporous Mesoporous Mater.* **2005**, *84*, 332−337.
(40) Lassinantti, M.; Jareman, F.; Hedlund, J.; Creaser, D.; Sterte, J. Preparation and evaluation of thin ZSM-5 membranes synthesized in the absence of organic template molecules. *Catal. Today* **2001**, *67*, 109−119.
(41) Zhou, M.; Liu, X.; Zhang, B.; Zhu, H. Assembly of oriented zeolite monolayers and thin films on polymeric surfaces via hydrogen bonding. *Langmuir* **2008**, *24*, 11942−11946.
(42) Krishna, R.; van Baten, J. M. Highlighting pitfalls in the Maxwell−Stefan modeling of water−alcohol mixture permeation across pervaporation membranes. *J. Membr. Sci.* **2010**, *360*, 476−482.
(43) Jentys, A.; Warecka, G.; Derewinski, M.; Lercher, J. A. Adsorption of water on ZSM 5 zeolites. *J. Phys. Chem.* **1989**, *93*, 4837−4843.
(44) Jentys, A.; Tanaka, H.; Lercher, J. Surface processes during sorption of aromatic molecules on medium pore zeolites. *J. Phys. Chem. B* **2005**, *109*, 2254−2261.
(45) Rege, S. U.; Yang, R. T. A novel FTIR method for studying mixed gas adsorption at low concentrations: $H_2O$ and $CO_2$ on NaX zeolite and $\gamma$-alumina. *Chem. Eng. Sci.* **2001**, *56*, 3781−3796.
(46) Bazin, P.; Alenda, A.; Thibault-Starzyk, F. Interaction of water and ammonium in NaHY zeolite as detected by combined IR and gravimetric analysis (AGIR). *Dalton Trans.* **2010**, *39*, 8432−8436.
(47) Olson, D.; Haag, W.; Borghard, W. Use of water as a probe of zeolitic properties: Interaction of water with HZSM-5. *Microporous Mesoporous Mater.* **2000**, *35*, 435−446.
(48) Bolis, V.; Busco, C.; Ugliengo, P. Thermodynamic study of water adsorption in high-silica zeolites. *J. Phys. Chem. B* **2006**, *110*, 14849−14859.
(49) Zhang, K.; Lively, R. P.; Noel, J. D.; Dose, M. E.; McCool, B. A.; Chance, R. R.; Koros, W. J. Adsorption of water and ethanol in MFI-type zeolites. *Langmuir* **2012**, *28*, 8664−8673.
(50) Yee, G. G.; Fulton, J. L.; Smith, R. D. Fourier transform infrared spectroscopy of molecular interactions of heptafluoro-1-butanol or 1-butanol in supercritical carbon dioxide and supercritical ethane. *J. Phys. Chem.* **1992**, *96*, 6172−6181.
(51) Lin-Vien, D.; Colthup, N. B.; Fateley, W. G.; Grasselli, J. G. *The Handbook of Infrared and Raman Characteristic Frequencies of Organic Molecules*; Elsevier: Amsterdam, Netherlands, 1991.
(52) Oudshoorn, A.; van der Wielen, L. A. M.; Straathof, A. J. Assessment of options for selective 1-butanol recovery from aqueous solution. *Ind. Eng. Chem. Res.* **2009**, *48*, 7325−7336.
(53) Zhang, K.; Zhang, L.; Jiang, J. Adsorption of $C_1$−$C_4$ alcohols in zeolitic imidazolate framework-8: Effects of force fields, atomic charges, and framework flexibility. *J. Phys. Chem. C* **2013**, *117*, 25628−25635.
(54) Einicke, W.; Messow, U.; Schöllner, R. Liquid-phase adsorption of *n*-alcohol/water mixtuers on zeolite NaZSM-5. *J. Colloid Interface Sci.* **1988**, *122*, 280−282.
(55) Zhu, W.; Van de Graaf, J.; Van den Broeke, L.; Kapteijn, F.; Moulijn, J. TEOM: A unique technique for measuring adsorption properties. Light alkanes in silicalite-1. *Ind. Eng. Chem. Res.* **1998**, *37*, 1934−1942.
(56) Sun, M. S.; Shah, D.; Xu, H. H.; Talu, O. Adsorption equilibria of $C_1$ to $C_4$ alkanes, $CO_2$, and $SF_6$ on silicalite. *J. Phys. Chem. B* **1998**, *102*, 1466−1473.
(57) Zhu, W.; Kapteijn, F.; Moulijn, J. Adsorption of light alkanes on silicalite-1: Reconciliation of experimental data and molecular simulations. *Phys. Chem. Chem. Phys.* **2000**, *2*, 1989−1995.
(58) Vlugt, T.; Krishna, R.; Smit, B. Molecular simulations of adsorption isotherms for linear and branched alkanes and their mixtures in silicalite. *J. Phys. Chem. B* **1999**, *103*, 1102−1118.
(59) Zhang, K.; Lively, R. P.; Dose, M. E.; Brown, A. J.; Zhang, C.; Chung, J.; Nair, S.; Koros, W. J.; Chance, R. R. Alcohol and water adsorption in zeolitic imidazolate frameworks. *Chem. Commun.* **2013**, *49*, 3245−3247.



DOI: 10.1021/acs.langmuir.5b00489
*Langmuir* 2015, 31, 4887−4894